Available online at www.sciencedirect.com
SCIENCE DIRECT®
Polyhedron 23 (2004) 2921–2928
POLYHEDRON
www.elsevier.com/locate/poly

Five-coordinate iron(II) complexes bearing tridentate nitrogen donor ligands as catalysts for atom transfer radical polymerisation

Rachel K. O'Reilly, Vernon C. Gibson *, Andrew J.P. White, David J. Williams

Department of Chemistry, Imperial College, Exhibition Road, South Kensington, London SW7 2AZ, UK

Received 27 May 2004; accepted 8 September 2004

Dedicated to Malcolm Green for his inspiring contributions to chemistry

Abstract

A series of five-coordinate complexes of iron(II) containing tridentate nitrogen donor ligands has been synthesised and evaluated for the atom transfer radical polymerisation of styrene. The molecular structures of two derivatives are described. Cyclic voltammetric studies show that the redox potential for the Fe(II)/Fe(III) couple strongly depends on the donor capacity of the complexing ligand, and styrene polymerisations reveal that ligands derived from alkyl amine or pyridine groups are the most active for ATRP, although slower than for their four-coordinate relatives due to unfavourable steric interactions. In general, catalyst activity decreases in the order of donor group: alkyl amine ≈ pyridine > alkyl imine ≫ aryl imine > aryl amine, with the aryl derivatives being almost completely inactive in ATRP. The trend in polymerisation activity correlates with the redox potential of the corresponding complexes. Complexes derived from aryl-imine or -amine ligands afford catalytic chain transfer rather than ATRP catalysis.

Keywords: Iron; Radical; Styrene; Catalyst; Polymerisation

1. Introduction

Atom transfer radical polymerisation (ATRP) allows the preparation of a wide range of well-defined polymeric materials with controlled molecular weights and complex architectures [1]. Following key reports by Matyjaszewski and Sawamoto in the mid-1990s, of highly efficient ATRP catalysts based on copper(I) and ruthenium(II) respectively, a number of different metal–ligand combinations have been investigated, including systems based on Rh, Pd, Ni and Fe [2–12]. There remains, however, a need to understand the factors important for efficient ATRP catalysis.

Since the process of ATRP is dependent upon the reversible binding of a halogen atom (Scheme 1), it is important that the metal complex has a relatively open coordination sphere, especially in its reduced form, and that neither the reduced nor the oxidised metal species are prone to decomposition. This may, for example, rule out three-coordinate complexes for many metals unless ligands are chosen that would stabilise the low coordination number. However, such ligands tend to be very bulky and not necessarily pre-disposed towards allowing the metal to accept another ligand.

Recently, we described a new family of four coordinate iron-based catalysts stabilised by α-diimine ligands [13,14]. These four-coordinate iron(II) complexes showed evidence for accessible and reversible redox couples to the corresponding iron(III) species depending on the nature of the imine substituents. The high catalytic

* Corresponding author. Tel.: +20 7594 5830; fax: +20 7594 5810.
E-mail address: v.gibson@imperial.ac.uk (V.C. Gibson).

0277-5387/$ - see front matter © 2004 Elsevier Ltd. All rights reserved.
doi:10.1016/j.poly.2004.09.001

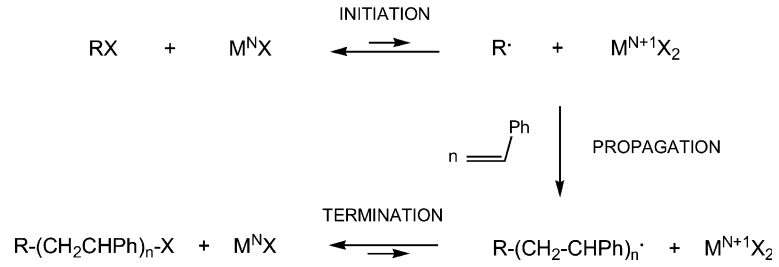

Scheme 1. Generalised mechanism for atom transfer radical polymerisation of styrene.

efficiency of these catalysts may be related to the fact that the reduced Fe(II) species possess a relatively uncluttered tetrahedral geometry and are, therefore, able to accept an additional halogen atom without any severe steric conflict arising between the co-ligands. In the five-coordinate oxidised form, the flexibility in the coordination geometry (via pseudo rotation) may assist the complex in achieving a coordination environment suited to the dissociation of a halogen atom (certain six-coordinate environments, e.g. d^3 and d^6 octahedral systems, have reduced kinetic lability). Thus, the 4–5 coordination manifold might be anticipated to possess important attributes for the efficient functioning of ATRP catalysts.

In order to further probe the effect of coordination geometry on the efficiency of ATRP catalysis, we decided to target a series of five-coordinate Fe(II) chloride complexes bearing tridentate nitrogen ligands and evaluate their performance in ATRP catalysis. These complexes possess an additional nitrogen donor relative to the (α-diimine)$FeCl_2$ catalysts reported recently, and would therefore be expected to afford lower oxidation potentials and render them more electronically suited to ATRP catalysis. However, these catalysts necessarily have to operate by interconverting between five- and six-coordinate species which may lead to increased steric conflict in the oxidised form of the catalyst.

Earlier work by Göbelt and Matyjaszewski examined tridentate bis(imino)pyridine and bis(amino)pyridine ligands bearing *N*-octyl substituents, in conjunction with copper(I) bromide and iron(II) bromide [15]. They found that the bis(imino)pyridine ligand formed an active catalyst in both systems, whereas, the bis(amino)pyridine ligand formed an active catalyst only in conjunction with copper(I) bromide. The use of bromide as the transferable group is recognised to hold advantages in terms of C–halogen bond strengths, though the thermodynamic advantage may be off-set by the increased steric demands of bromine atoms coordinated to the metal centre. In this study we focus on a series of metal–chloride derivatives containing tridentate ligands with a view to obtaining an improved understanding of the factors influencing efficient ATRP catalysis in iron-based systems.

2. Results and discussion

2.1. Synthesis and characterisation

The series of tridentate [NNN] ligands, **I**–**VI**, containing a central pyridine or amine unit and two peripheral imine or amine donors with either *N*-alkyl or *N*-aryl substituents was synthesised (Fig. 1). Ligand **I** (PMDETA) is commercially available, while **II**, **III**, **V** and **VI** were synthesised using literature procedures[16–21]. Ligand **IV** was synthesized by a modification of a literature preparation using $Si(OEt)_4$ and recovered as a yellow solid in 62% yield [22]. Ligands **I**–**VI** were reacted with iron(II) dichloride to afford the corresponding monochelate complexes (**1**–**6**) in good yields.

Complexation of **I** to iron(II) dichloride was first reported in 1966, by Ciampolini and Speroni [23]. At that time, **1** was the first reported high spin five-coordinate iron(II) complex. In 1999, Calderazzo and co-workers [24] structurally characterized **1** and reported a distorted square pyramidal structure with a chlorine atom occupying the apical position. Ligand **II** has previously been

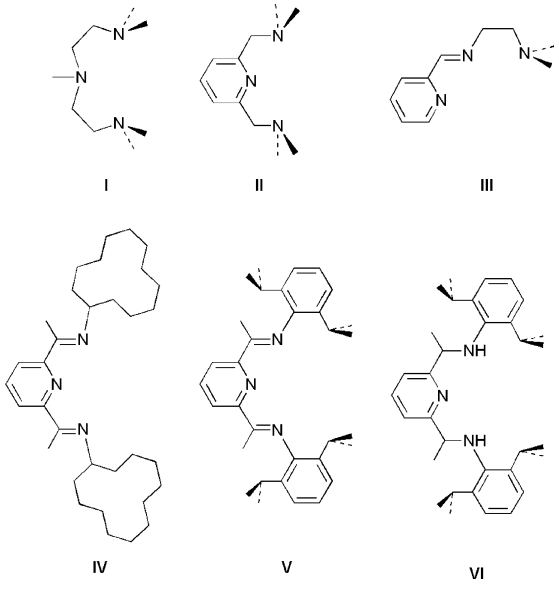

Fig. 1. Ligands **I**–**VI**.

complexed to mid and late transition metals such as ruthenium and zinc by the groups of van Koten and Reinhoudt [18,25]. It was synthesised by reaction of 2,6-bis(bromomethyl)pyridine with dimethylamine and complexed to iron(II) to afford **2**, as a yellow microcrystalline solid. Single crystals of **2** were grown by slowly cooling a saturated solution of **2** in hot tetrahydrofuran. X-ray single crystal analysis revealed the structure (which has molecular C_S symmetry about a plane containing the iron, the two chlorides and the pyridine nitrogen atom) to have a distorted square pyramidal geometry around the iron centre (Fig. 2). The four basal atoms {Cl(1),N(1),N(7),N(8)} are coplanar to within 0.06 Å with the iron lying ca. 0.68 Å out of this plane in the direction of the apical atom Cl(2); the *trans*-basal angles are 136.1(2) and 147.0(2)°, and the apical–basal angles range between 106.2(2) and 111.4(2)°. The Fe–Cl bond lengths are noticeably asymmetric, with that to the apical chloride being significantly shorter [2.291(2) Å] than to its basal counterpart [2.341(2) Å]; the Fe–N distances are unexceptional [21,24,26]. The two five-membered chelate rings both have envelope geometries with in each case the amino nitrogen lying out of the plane of the other four atoms [by ca. 0.57 Å for N(7) and ca. 0.68 Å for N(8)] which are coplanar to within 0.02 Å. The only intermolecular packing interaction of note is a π–π stacking between adjacent pyridyl rings with centroid···centroid and mean interplanar separations of 3.72 and 3.55 Å, respectively. Subsequent to this determination, Grubbs and co-workers [27] reported the room temperature (298 K) structure of the same polymorph of **2** in a private communication; taking into account the 115 K difference in temperature, the unit cells are the same.

Ligand **III** has recently been complexed to late transition metals such as copper and palladium [28,29]. Complex **3** was synthesised by reaction of **III** with iron(II) dichloride in diethyl ether and was isolated as a dark red, microcrystalline solid. This complex was first reported in 1969 and, based on magnetic and spectroscopic techniques, a five-coordinate geometry around the iron centre was proposed [30]. We confirmed this assignment by determining the solid state X-ray structure of crystals of **3** obtained by slow diffusion of an equal volume of heptane into a saturated solution of **3** in dichloromethane. This study revealed **3** to have a structure (Fig. 3) closely related to that of its zinc dibromide analogue [31]. The geometry at iron can be considered as intermediate between square pyramidal, with Cl(2) occupying the apical position, and trigonal bipyramidal with N(1) and N(10) defining the major axis, though being somewhat closer to the latter description. Considered as square pyramidal, the metal centre lies ca. 0.58 Å [0.64 Å] out of the basal plane which is only coplanar to within 0.18 Å [0.30 Å]. Viewed as trigonal bipyramidal, the axial atoms subtend an angle of 147.21(14)° [150.2(2)°] at the metal, and the angles within the equatorial plane range between 108.30(11) and 141.54(11)° [111.8(2) and 133.9(2)°]; the iron lies ca. 0.06 Å [0.04 Å] out of the equatorial plane in the direction of N(10). (The values in square parentheses refer to the zinc dibromide analogue [31].) The five-membered N(1)/N(7) chelate ring is almost planar with the metal lying ca. 0.09 Å [<0.01 Å] out of the plane of the other four atoms which are coplanar to better than 0.01 Å. By contrast, the N(7)/N(10) five-membered chelate ring has a twisted envelope conformation with N(10) displaced by ca. 0.72 Å [0.76 Å] out of the plane of the other atoms, which are coplanar to within 0.08 Å [0.12 Å]. The pattern of bonding around the metal centre is generally the same between the $FeCl_2$ species **3** and its previously reported $ZnBr_2$ analogue, though it is noticeable that, whereas in the $ZnBr_2$ complex the M–N(pyridyl) and M–N(amino) distances are the same [2.245(8) and

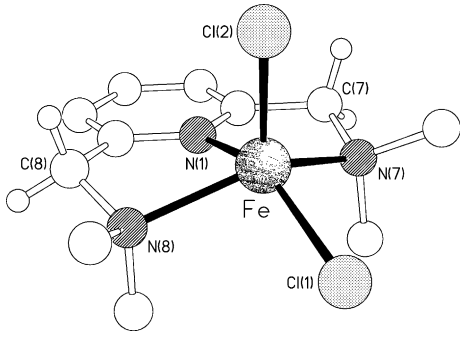

Fig. 2. The molecular structure of **2**. Selected bond lengths (Å) and angles (°); Fe–Cl(1) 2.341(2), Fe–Cl(2) 2.291(2), Fe–N(1) 2.121(6), Fe–N(7) 2.262(6), Fe–N(8) 2.248(6), C(7)–N(7) 1.468(9), C(8)–N(8) 1.474(10), N(1)–Fe–N(8) 74.3(2), N(1)–Fe–N(7) 74.4(2), N(8)–Fe–N(7) 136.1(2), N(1)–Fe–Cl(2) 106.2(2), N(8)–Fe–Cl(2) 106.4(2), N(7)–Fe–Cl(2) 111.4(2), N(1)–Fe–Cl(1) 147.0(2), N(8)–Fe–Cl(1) 95.7(2), N(7)–Fe–Cl(1) 94.1(2), Cl(2)–Fe–Cl(1) 106.84(9).

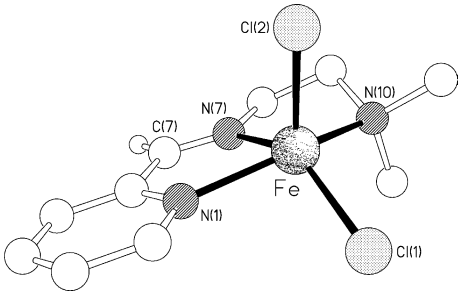

Fig. 3. The molecular structure of **3**. Selected bond lengths (Å) and angles (°); Fe–Cl(1) 2.3034(12), Fe–Cl(2) 2.3361(13), Fe–N(1) 2.185(4), Fe–N(7) 2.129(3), Fe–N(10) 2.236(4), C(7)–N(7) 1.258(6), N(7)–Fe–N(1) 74.04(14), N(7)–Fe–N(10) 75.98(14), N(1)–Fe–N(10) 147.21(14), N(7)–Fe–Cl(1) 141.54(11), N(1)–Fe–Cl(1) 93.79(10), N(10)–Fe–Cl(1) 101.55(10), N(7)–Fe–Cl(2) 108.30(11), N(1)–Fe–Cl(2) 102.39(10), N(10)–Fe–Cl(2) 99.34(11), Cl(1)–Fe–Cl(2) 109.94(5).

2.236(7) Å, respectively], in **3** the M–N(pyridyl) bond length is noticeably shorter [2.185(4) Å] than that to the amino nitrogen [2.236(4) Å]. The Fe–N bond lengths differ noticeably from those in, for example, (2-((2,6-di-*iso*propylphenyl)iminomethyl)-6-(1-(2,6-di-*iso*propylphenylamino)ethyl)pyridine-*N*,*N*′,*N*″)dichloroiron(II) and other related complexes with the bond to the pyridine nitrogen being longer and that to the imino nitrogen shorter [25]. The Fe–Cl bond lengths in **3** are noticeably asymmetric, with that to the pseudo-apical chloride Cl(2) being significantly longer [2.3661(13) Å] than to its pseudo-basal counterpart Cl(1) [2.3034(12) Å]. The only intermolecular packing feature of note is a π–π stacking of the pyridine rings of centrosymmetrically related pairs of molecules; the centroid···centroid and mean interplanar separations are 3.54 and 3.38 Å, respectively. An analogous contact is seen in the zinc dibromide species with centroid–centroid and mean interplanar separations of 3.56 and 3.36 Å, respectively.

Complex **4** was synthesized by a similar route to that reported in the literature for the *N*-aryl derivative, **5** [32]. After washing with diethyl ether and extraction into tetrahydrofuran, **4** was isolated as a dark grey microcrystalline solid. The *N*-aryl pyridine(bis)imino and pyridine(bis)amino complexes, **5** and **6**, have both been reported recently by this group and were synthesized as described in the literature reports [32,33]. Both of these complexes have previously been structurally characterized and found to possess a five-coordinate distorted square pyramidal geometry.

Complexes **1**–**6** are all air-stable paramagnetic solids, with magnetic moments (determined by the Evans' NMR method) in the range 4.9–5.3 μ_B [34–36]. The magnetic moments are consistent with the presence of four unpaired electrons and a quintet ground state ($S = 2$) for the iron(II) centres [37].

2.2. Cyclic voltammetry

Matyjaszewski and co-workers [38] have investigated the structure–activity relationship for a series of tridentate nitrogen donor ligands in copper-based ATRP. The redox properties of these complexes were measured using CV techniques and their electrochemistry was correlated to their activity as ATRP catalysts for styrene and MMA polymerisation [39]. By comparison with Matyjaszewski's findings in copper-based ATRP, it would be predicted that the series of complexes should exhibit the following order of reducing power: **1** < **2** < **3** < **4** ≪ **5** < **6**. Experimentally determined electrochemical parameters for **1**–**6** are collected in Table 1 and confirm this trend. Table 1 also shows the oxidation potentials, E_{ox}, for this series of complexes. Since this parameter can be correlated with the ease of oxidation of the complex, E_{ox} should provide an indication of activities in ATRP catalysis.

Table 1
Cyclic voltammetry results for **1**–**6**

	E_{ox} (mV)	$E_{1/2}$ (mV)	ΔE_p (mV)
1	−370	−280	170
2	−240	−150	170
3	−190	−100	180
4	−150	−70	170
5	180	330	310
6	260	410	320

Complexes **1**–**4** all have low oxidation potentials (−370 to −150 mV) and redox potentials (−280 to −70 mV) indicating that they are easy to oxidise, unlike **5** and **6** whose high oxidation potentials indicate the opposite. Thus, it would be predicted that **1**–**4** should be active ATRP catalysts since they are easily oxidised and possess an accessible and reversible one-electron redox couple. In fact, **1**–**4** have lower redox potentials than the previously reported *N*-alkyl diimine complexes ($E_{1/2}$ ca.−100 mV) and thus would be predicted to be faster ATRP catalysts [13]. However, **5** and **6**, which are supported by ligands possessing *N*-aryl groups have irreversible ($\Delta E_p > 300$ mV) and less accessible ($E_{1/2} > 300$ mV) redox couples and thus would be predicted to have low activity in ATRP.

2.3. Polymerisation results

Complexes **1**–**6** were screened for the ATRP of styrene (200 equiv.) at 120 °C using 1-phenylethyl chloride (1-PECl) as an initiator and the results are presented in Table 2. **1**–**4** polymerised styrene in a controlled manner, with linear kinetics and with molecular weights increasing with monomer conversion [40]. Analysis of the polymer produced using **1**–**4** revealed the presence of a halogen end group by ^{1}H NMR spectroscopy and also by microanalysis [for **2**, M_n = 5100% Cl, found (calc.): 0.64 (0.70)]. The more reducing the complex, the lower the redox potential, and the faster the ATRP catalyst cf. **1** versus **3** (Fig. 4).

However, these complexes are slower ATRP catalysts than their α-diimine counterparts (e.g. for 1,2-bis(cyclo-

Table 2
Results of styrene polymerisations using **1**–**6**

	k_{obs} (h^{-1})	% Conv. in 24 h	$M_{n,calc}$[a]	M_n	M_w/M_n
1	0.04	65	13700	15100	1.62
2	0.03	52	10900	11800	1.53
3	0.02	39	8200	8500	1.59
4	0.02	37	7800	8700	1.56
5		72	15100	2900	2.07
6		45	9500	2100	1.92

Conditions: 120 °C, bulk, $[1\text{-PECl}]_0$:$[\text{catalyst}]_0$:$[\text{styrene}]_0$ = 1:1:200. Control polymerisation of styrene at 120 °C with no catalyst > 90% conversion in 24 h, M_n ca. 200000.

[a] $M_{n,calc}$ is calculated M_n based on degree of conversion.

hexylimino)ethane iron(II) dichloride, $k_{obs} = 0.25\ h^{-1}$, cf. $k_{obs} = 0.04\ h^{-1}$ for **1**), despite their significantly lower redox potentials (for 1,2-bis(cyclohexylimino)ethane iron(II) dichloride, $E_{1/2} = -120$ mV cf. $E_{1/2} = -280$ mV for **1**) [13]. This can be attributed to the less favourable steric environment around the metal in these five-coordinate complexes as compared with the four-coordinate tetrahedral α-diimine complexes. Thus, the rate of Cl atom transfer from RCl to **1**, for example, is slowed due to steric crowding, despite **1** having more favourably disposed redox chemistry. This may also explain the loss of control and broadening of the polydispersity of the polymers produced using these five-coordinate systems compared to their α-diimine relatives.

For **5** and **6**, which both possess *N*-aryl substituents, the polymerisation did not proceed in a controlled manner and low molecular weight polymers were produced throughout, the molecular weight of which were independent of the degree of conversion (Fig. 5). The polymer produced had unsaturated end groups by ^{1}H NMR spectroscopy and zero halide content by microanalysis. Thus, complexes **5** and **6** do not polymerize styrene by an ATRP mechanism, but rather chain propagation is accompanied by catalytic chain transfer (CCT). Here, the polystyrenyl radical reacts with the Fe(II) catalyst to generate an organometallic Fe(III) species which undergoes β-hydrogen elimination to release the polymer chain bearing an unsaturated end-group. This is presumed to occur in an analogous manner to that proposed for the α-diimine catalyst system shown in Scheme 2 [14]. The capacity of the aryl derivatives to support CCT, we believe, is a result of a lower spin ($S = 3/2$) ground state for the oxidised Fe(III) species containing aryl substituents (the alkyl derivatives are all high spin) affording stronger Fe–C bonds and consequently more stable organometallic intermediates.

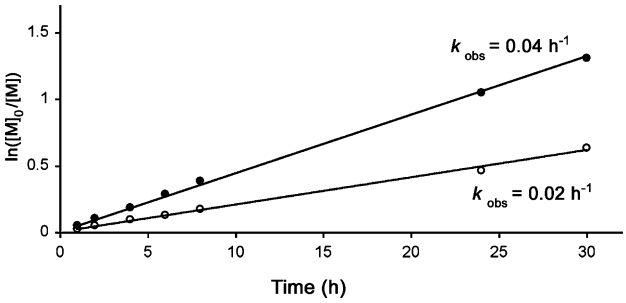

Fig. 4. Plot of $\ln([M]_0/[M])$ vs. time for complexes **1** (•) and **3** (○).

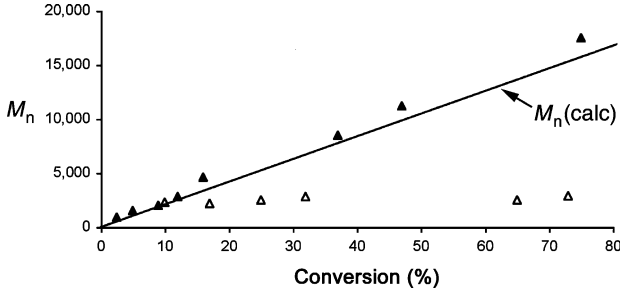

Fig. 5. Plot of M_n vs. conversion for **4** (▲) and **5** (Δ).

3. Conclusions

Iron(II) dichloride complexes containing neutral tridentate [NNN] ligands are found to be active ATRP catalysts, and their activities correlate well with their oxidation potentials. Although their electrochemical properties suggest that they should be more efficient catalysts than four-coordinate α-diimine iron systems, they are in fact much slower. This is explained by the increased steric hindrance at the metal for the oxidised six-coordinate species, which prevents fast and facile atom transfer from occurring. Thus the hypothesis made

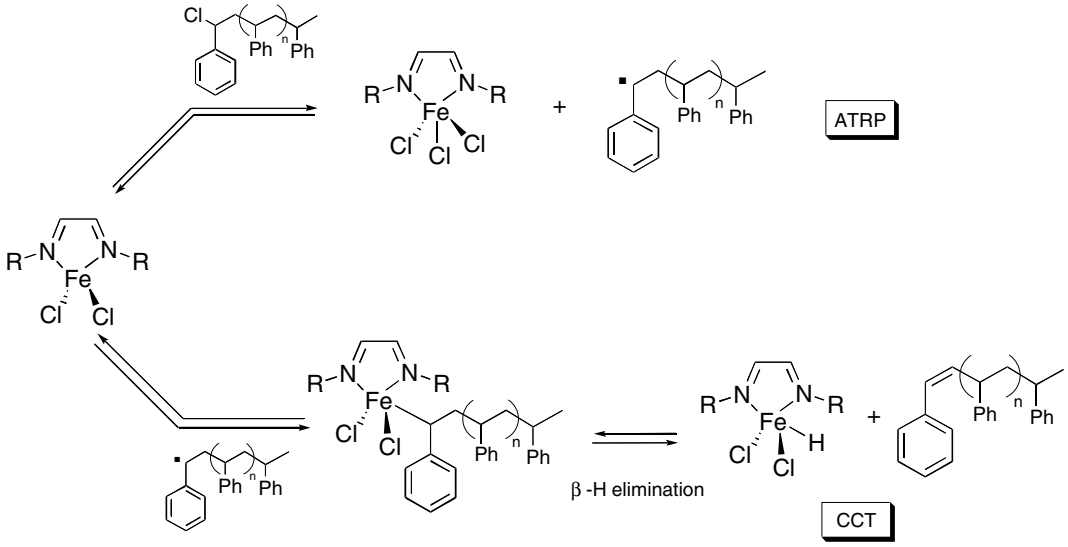

Scheme 2. ATRP vs. CCT pathways for α-diimine iron catalysts.

at the outset of this study, that a four/five-coordinate equilibrium should be more favourable than a five/six-coordinate equilibrium for efficient ATRP catalysis in iron complexes appears to hold.

4. Experimental

4.1. General

All manipulations of water and/or moisture sensitive compounds were performed by means of standard high vacuum Schlenk and cannula techniques. Air sensitive compounds were transferred to a nitrogen filled glovebox and, unless stated otherwise, stored at room temperature. Crystal data were collected on Siemens P4/PC or P4/RA diffractometers. NMR spectra were recorded on a Bruker AC-250 MHz, DRX-400 MHz or AM-500 MHz spectrometers. Infra-red spectra were obtained with thin sample films on NaCl plates or as KBr discs on a Perkin–Elmer 1710X FT-IR spectrometer. Mass spectra were recorded on either a VG Autospec or a VG Platform II spectrometer. Elemental analyses were performed by the microanalytical services of the Chemistry departments of London Metropolitan University and University College London. Magnetic susceptibilities were determined by the Evans NMR method. Gel permeation chromatography (GPC) was performed using Viscotek Trisec software connected to a Knauer differential refractometer. Samples were injected onto two linear 10 μm columns using chloroform as elutant (conventionally calibrated prior to use, using polystyrene standards (PSS Mainz)) at a flow rate of 1.0 $cm^3 min^{-1}$ at room temperature. Cyclic voltammetry (CV) was performed using a MacLab potentiostat operated by EChem 1.3.2. software. The working electrode and reference electrode were purchased from Bioanalytical (ref: MF-2013 and RE-5B).

All solvents were dried by prolonged reflux over a suitable drying agent under an atmosphere of nitrogen, being freshly distilled prior to use. All solvents were degassed prior to use unless otherwise stated. Styrene (St) was purified by vacuum distillation and then stored under an inert atmosphere over 4 Å molecular sieves at −15 °C. 1-PECl was synthesized according to literature methods and purified by column chromatography [41]. All amines and anilines were freshly distilled before use. All other reagents are commercially available and were used without further purification. Compounds **1**[23] **5**[21] and **6**[33] were prepared by literature procedures.

All polymerisations were set up and performed under an atmosphere of oxygen-free, dry dinitrogen using standard Schlenk-line techniques. In an ampoule equipped with a magnetic stirrer bar, were placed in order, monomer, initiator and catalyst in various ratios and the ampoule was then sealed. In all cases the catalyst was soluble in the monomer solution. The ampoules were heated in an oil bath, at 120 °C. After stirring for the allotted period of time, an aliquot (0.1 ml) was removed and quenched with THF (1 ml). Conversion was determined by integration of the monomer versus polymer backbone resonances in the ^1H NMR spectrum of the crude product in $CDCl_3$. After the reaction time, usually 24 h, the contents of the ampoules were dissolved in THF. This solution was added dropwise to an approximately 20-fold excess of rapidly stirred acidified methanol (1% HCl v/v). The precipitate that formed was filtered off and washed with methanol. The precipitate was dried for 24 h in a vacuum oven at 60 °C. Samples were then analysed by GPC.

CV was performed using a sample vial (50 × 24 mm) as a cell. The counter electrode was a section of 0.5 mm platinum wire, the working electrode was a platinum disk electrode and the reference electrode was a Ag/AgCl electrode. Electrolyte ($[^nBu_4N][PF_6]$ (1.00 mmol)) and the complex under study (0.01 mmol) was loaded into the cells before being degassed by evacuation and admission of dinitrogen, acetonitrile (10 cm^3) was then added.

4.2. Preparation of 2,6-bis-[(dimethylamino)methyl]-pyridine) (*II*)

Dimethylamine (6.0 g, 0.133 mol) was quickly added to 30 ml of precooled (ca. 5 °C) C_6H_6 after which a solution of 2,6-bis(bromomethyl)pyridine (3.51 g, 0.013 mol) in 80 ml of C_6H_6 was added dropwise over 30 minutes [12,13]. After stirring at room temperature for 30 min, the reaction mixture was filtered under suction and the residue was washed with Et_2O. The C_6H_6 and Et_2O fractions were combined and reduced in vacuo to yield a pale yellow oil. This oil was vacuum distilled at 60 °C and 8 mm/Hg to afford a colourless oil (2.45 g, 95%). *Anal.* Calc. for $C_{11}H_{19}N_3$: C, 68.4; H, 9.9; N, 21.7. Found: C, 67.7; H, 9.5; N, 21.7%. δ_H ($CDCl_3$) 7.50 (1H, t, *J*(HH) 8 Hz, 1Ar–*H*), 7.15 (2H, d, *J*(HH) 8 Hz, 2Ar–*H*), 3.46 (4H, m, 2CH_2), 2.15 (12H, s, 4CH_3); δ_C (CD_3COCD_3) 159.6 (s, 2Ar–*C*), 137.3 (s, 1Ar–*C*), 121.5 (s, 2Ar–*C*), 66.5 (s, 2*C*H_2), 45.9 (s, 4*C*H_3); MS (CI^+) (*m*/*z*) 194 $[M+H]^+$.

4.3. Preparation of 2,6-bis-(cyclododecylimino)pyridine (*IV*)

A solution of 2,6-diacetylpyridine (5.0 g, 0.03 mol) and cyclododecylamine (13.8 g, 0.075 mol) in $Si(OEt)_4$ (14.05 g, 0.067 mol) with a few drops of concentrated H_2SO_4 was placed in a round bottom flask and attached to a side arm and air condenser which was stoppered with a round bottom flask [18]. The solution was heated overnight with stirring at 130 °C, after which time etha-

nol (ca. 3 ml) had been distilled over from the reaction mixture. The solid reaction mixture was dissolved in CH_2Cl_2, washed with saturated solutions of $NaHCO_3$ (2×10 ml) and brine (2×10 ml) and then dried over $MgSO_4$. The solvent was removed in vacuo to afford a yellow solid. Washing this solid with cold petroleum ether (20 ml) afforded ligand **IV** as a bright yellow solid (9.17 g, 62%). *Anal.* Calc. for $C_{35}H_{55}N_3$: C, 80.3; H, 11.2; N, 8.5. Found: C, 79.6; H, 11.1; N, 8.7%. IR/cm^{-1} (C=N) 1650s; δ_H ($CDCl_3$) 8.03 (2H, d, *J*(HH) 8 Hz, 2Ar-*H*), 7.66 (1H, t, *J*(HH) 8 Hz, Ar–*H*), 3.82 (2H, m, 2C*H*), 2.41 (6H, s, 2CH_3), 1.58–1.25 (44H, br m, 22CH_2); δ_C ($CDCl_3$) 163.9 (s, 2Ar–*C*), 156.7 (s, 2Ar–*C*), 136.4 (s, Ar–*C*), 121.1 (s, 2Ar–*C*), 57.04 (s, 2*C*H), 40.35 (s, 2*C*H_3), 24.7–21.3 (s, 22*C*H_2); MS (CI^+) (*m*/*z*) 494 $[M+H]^+$.

4.4. Preparation of 2,6-bis-[(dimethylamino)methyl]-pyridine) iron(II) chloride (2)

To a solution of $FeCl_2(THF)_{1.5}$ (0.58 g, 0.0025 mol) in toluene (20 ml) was added dropwise, with stirring, ligand **II** (0.48 g, 0.0025 mol) also in toluene (20 ml) and the resulting suspension stirred overnight at room temperature. The mixture was then cooled to 0 °C and filtered; the filtrate was reduced to ca. 10 ml and stored overnight at −10 °C, after which time crystals of **2** had formed. These yellow crystals were isolated by filtration and dried overnight in vacuo. This afforded **2** as a microcrystalline bright yellow solid (0.67 g, 84%). Slow cooling of a solution of **2** in hot THF afforded crystals suitable for X-ray analysis. *Anal.* Calc. for $C_{11}H_{19}N_3Cl_2Fe$: C, 41.2; H, 6.0; N, 13.1. Found: C, 41.2; H, 6.0; N, 13.0%. IR/cm^{-1} 3584m, 3397s, 2349w, 2282w, 1653m, 1559w, 1541w, 1507w, 1457w, 1073w, 666w; MS (CI^+) (*m*/*z*) 319 $[M]^+$; μ_{eff} = 5.05 μ_B.

4.5. Preparation of N,N-dimethyl-N′-pyridin-2-ylmethylene-ethane-1,2-diamino iron(II) chloride (3)

To a suspension of $FeCl_2$ (1.27 g, 0.01 mol) in Et_2O (20 ml) was added dropwise, with stirring *N*,*N*-dimethyl-*N*′-pyridin-2-ylmethylene-ethane-1,2-diamine, **III** (1.77 g, 0.01 mol) in Et_2O (10 ml) [24]. The reaction mixture was stirred overnight at room temperature and then filtered and the filtrate reduced under reduced pressure. The solid residue was extracted into CH_2Cl_2 and then the solvent was removed. The resultant solid was dried in vacuo and this afforded **3** as a purple microcrystalline solid (2.01 g, 66%). Slow diffusion of a solution of **3** in $CH_2Cl_2$with an equal volume of heptane afforded crystals suitable for X-ray analysis. *Anal.* Calc. for $C_{10}H_{15}N_3Cl_2Fe$: C, 39.5; H, 5.0; N, 13.8. Found: C, 39.1; H, 5.0; N, 13.2%. IR/cm^{-1} 3447m, 2966m, 2838w, 1615w, 1568m, 1507w, 1457w, 1279w, 1174w, 1117w, 1026w, 923w, 750w; MS (CI^+) (*m*/*z*) 318 $[M+NH_4]^+$; μ_{eff} = 4.96 μ_B.

4.6. Preparation of 2,6-bis-(cyclododecylimino)pyridine iron(II) chloride (4)

To a suspension of $FeCl_2$ (0.92 g, 0.007 mol) in ^{n}BuOH (20 ml) was added dropwise, with stirring, **IV** (4 g, 0.008 mol) also in ^{n}BuOH (10 ml) and the reaction mixture stirred overnight at 90 °C. After this time it was allowed to cool and the solvent was then removed in vacuo at 60 °C for 4 h. The residue was washed with Et_2O (3×10 ml) and then extracted into THF (20 ml). The solution was reduced to ca. 10 ml and stored at −10 °C overnight. After this time, dark grey crystals of **4** had formed which were isolated by filtration and dried (3.30 g, 73%). *Anal.* Calc. for $C_{33}H_{55}N_3Cl_2Fe$: C, 63.9; H, 8.9; N, 6.8; Cl, 11.4. Found: C, 63.7; H, 8.7; N, 6.8; Cl, 10.3%. IR/cm^{-1} 2938s, 2864s, 2362w, 1703m, 1585w, 1470m, 1446m, 1359w, 1292w, 1268w, 1205w, 1163w, 1075w, 1020w, 994w, 813w, 740w; MS (FAB^+) (*m*/*z*) 584 $[M-Cl]^+$; μ_{eff} = 5.11 μ_B.

4.7. X-ray crystallography

Crystal data for **2**: $C_{11}H_{19}N_3Cl_2Fe$, M = 320.04, tetragonal, $P4_32_12$ (no. 96), a = 10.5887(5), c = 26.080(3) Å, V = 2924.1(4) Å^3, Z = 8, D_c = 1.454 gcm^{-3}, μ(Cu Kα) = 11.491 mm^{-1}, T = 183 K, yellow platy prisms; 2142 independent measured reflections, F^2 refinement, R_1 = 0.054, wR_2 = 0.122, 1720 independent observed absorption-corrected reflections [$|F_o| > 4\sigma(|F_o|)$, $2\theta_{max}$ = 120°], 155 parameters. The absolute structure of **1** was determined by a combination of *R*-factor tests [$R_1^+ = 0.0541$, $R_1^- = 0.1025$] and by use of the Flack parameter [$x^+ = -0.013(14)$]. CCDC 239659.

Crystal data for **3**: $C_{10}H_{15}N_3Cl_2Fe\cdot0.5CH_2Cl_2$, M = 346.46, monoclinic, I 2/*a* (no. 15), a = 14.870(3), b = 10.2360(8), c = 20.545(4) Å, β = 104.216(11)°, V = 3031.4(9) Å^3, Z = 8, D_c = 1.518 gcm^{-3}, μ(Mo Kα) = 1.508 mm^{-1}, T = 293 K, very dark red/brown needles; 2666 independent measured reflections, F^2 refinement, R_1 = 0.046, wR_2 = 0.103, 2011 independent observed absorption-corrected reflections [$|F_o| > 4\sigma(|F_o|)$, $2\theta_{max}$ = 50°], 173 parameters. CCDC 239660.

5. Supplementary material

Full crystallographic details have been deposited in CIF format with the Cambridge Crystallographic Data Centre. Copies of this information may be obtained free of charge from The Director, CCDC, 12 Union Road, Cambridge, CB2 1EZ, UK (fax: +44 1223 336033; e-mail: deposit@ccdc.cam.ac.uk or www: http//www.ccdc.cam.ac.uk).

Acknowledgements

BP Chemicals is thanked for financial support (R.K. O'R). Dr. Jane Boyle is thanked for NMR measurements.

References

[1] (a) For recent reviews see K. Matyjaszewski, J. Xia, Chem. Rev. 101 (2001) 2921;
(b) M. Kamigaito, T. Ando, M. Sawamoto, Chem. Rev. 101 (2001) 3689.
[2] J.S. Wang, K. Matyjaszewski, J. Am. Chem. Soc. 117 (1995) 5614.
[3] M. Kato, M. Kamigaito, M. Sawamoto, T. Higashimura, Macromolecules 28 (1995) 1721.
[4] P. Lêcomte, I. Drapier, P. Dubois, P. Teyssié, R. Jérôme, Macromolecules 30 (1997) 7631.
[5] G. Moineau, C. Granel, P. Dubois, P. Teyssié, R. Jérôme, Macromolecules 31 (1998) 542.
[6] C. Granel, P. Dubois, R. Jêromé, P. Teyssié, Macromolecules 29 (1996) 8576.
[7] T. Ando, M. Kamigaito, M. Sawamoto, Macromolecules 30 (1997) 4507.
[8] K. Matyjaszewski, M. Wei, J. Xia, N.E. McDermott, Macromolecules 30 (1997) 8161.
[9] K. Matyjaszewski, S. Coca, S.G. Gaynor, M. Wei, B.E. Woodworth, Macromolecules 30 (1997) 7348.
[10] M. Teodorescu, S.G. Gaynor, K. Matyjaszewski, Macromolecules 33 (2000) 2335.
[11] T. Sarbu, K. Matyjaszewski, Macromol. Chem. Phys. 202 (2001) 3379.
[12] V.C. Gibson, R.K. O'Reilly, D.F. Wass, A.J.P. White, D.J. Williams, J. Chem. Soc., Dalton Trans. (2003) 2824.
[13] V.C. Gibson, R.K. O'Reilly, D.F. Wass, W. Reed, A.J.P. White, D.J. Williams, Chem. Commun. (2002) 1850.
[14] V.C. Gibson, R.K. O'Reilly, D.F. Wass, A.J.P. White, D.J. Williams, Macromolecules 36 (2003) 2591.
[15] B. Göbelt, K. Matyjaszewski, Macromol. Chem. Phys. 201 (2000) 1619.
[16] M. Newcomb, J.M. Timko, D.M. Walba, D.J. Cram, J. Am. Chem. Soc. 99 (1977) 6392.
[17] B.A. Markies, P. Wijkens, J. Boersma, H. Kooijman, N. Veldman, A.L. Spek, G. van Koten, Organometallics 13 (1994) 3244.
[18] P. Molenveld, W.M.G. Stikvoort, H. Koojiman, A.L. Spek, J.F.J. Engbersen, D.N. Reinhoudt, J. Org. Chem. 64 (1999) 3896.
[19] G. Zahrzewski, G.P. Speroni, Inorg. Chem. 7 (1968) 1034.
[20] F. Guérin, D.H. Mc Conville, J.J. Vittal, Organometallics 15 (1996) 5586.
[21] G.J.P. Britovsek, M. Bruce, V.C. Gibson, B.S. Kimberley, P.J. Maddox, S. Mastroianni, S.J. McTavish, C. Redshaw, G.A. Solan, S. Strömberg, A.J.P. White, D.J. Williams, J. Am. Chem. Soc. 121 (1999) 8728.
[22] B.E. Love, J. Ren, J. Org. Chem. 58 (1993) 5556.
[23] M. Ciampolini, G.P. Speroni, Inorg. Chem. 5 (1966) 45.
[24] F. Calderazzo, U. Englert, G. Pampaloni, E. Vanni, C.R. Acad. Sci. Paris (1999) 311.
[25] I. Del Rio, R.A. Gossage, M.S. Hannu, M. Lutz, A.L. Spek, G. van Koten, Organometallics 18 (1999) 1097.
[26] B.L. Small, M. Brookhart, A.M.A. Bennett, J. Am. Chem. Soc. 120 (1998) 4049.
[27] M.W. Day, B.D. Ward, R.H. Grubbs, Private Communication, CCDC OCUJOL (2001).
[28] M. Costa, P. Pelagatti, C. Pelizzi, D. Rogolino, J. Mol. Catal. A 178 (2002) 21.
[29] P.S. Mukherjee, T.K. Maji, A. Escuer, R. Vicente, J. Ribas, G. Rosair, F.A. Mautner, N.R. Chaudhuri, Eur. J. Inorg. Chem. (2002) 943.
[30] P. Bamfield, R. Price, R.G.J. Millar, J. Chem. Soc. A 9 (1969) 1447.
[31] G. Zakrzewski, E.C. Lingafelter, Inorg. Chim. Acta 4 (1970) 251.
[32] G.J.P. Britovsek, V.C. Gibson, B.S. Kimberley, P.J. Maddox, S.J. McTavish, G.A. Solan, A.J.P. White, D.J. Williams, Chem. Commun. (1998) 849.
[33] G.J.P. Britovsek, V.C. Gibson, S. Mastroianni, D.C.H. Oakes, C. Redshaw, G.A. Solan, A.J.P. White, D.J. Williams, Eur. J. Inorg. Chem. (2001) 431.
[34] D.F. Evans, J. Chem. Soc. (1959) 2003.
[35] D.F. Evans, G.V. Fazakerley, R.F.J. Phillips, J. Chem. Soc. A (1971) 1931.
[36] D.H. Grant, J. Chem. Ed. 72 (1995) 39.
[37] B.N. Figgis, J. Lewis, in: J. Lewis, R.G. Wilkins (Eds.), Modern Coordination Chemistry, Interscience, New York, 1960, p. 400.
[38] K. Matyjaszewski, B. Göbelt, H.-J. Paik, C.P. Horwitz, Macromolecules 34 (2001) 430.
[39] J. Qui, K. Matyjaszewski, L. Thouin, C. Amatore, Macromol. Chem. Phys. 201 (2000) 1625.
[40] A. Goto, T. Fukuda, Prog. Polym. Sci. 29 (2004) 329.
[41] D. Landini, F. Rolla, J. Org. Chem. 45 (1980) 3527.